AGU PUBLICATIONS

Water Resources Research

RESEARCH ARTICLE

10.1002/2012WR012922

Special Section:
New Modelling Approaches and Novel Experimental Technologies for Improved Understanding of Process Dynamics at Aquider-Surface Water Interfaces

River-aquifer interactions in a semiarid environment investigated using point and reach measurements

Andrew M. McCallum[1], Martin S. Andersen[1,2], Gabriel C. Rau[1,2], Joshua R. Larsen[2,3], and R. Ian Acworth[1,2]

[1]Connected Waters Initiative Research Centre, Water Research Laboratory, School of Civil and Environmental Engineering, UNSW Australia, Sydney, New South Wales, Australia, [2]National Centre for Groundwater Research and Training, UNSW Australia, Sydney, New South Wales, Australia, [3]School of Geography, Planning, and Environmental Management, University of Queensland, St Lucia, Queensland, Australia

Key Points:
- Losing riverbed fluxes under high flows and approximately neutral under low flows
- Event driven riverbed fluxes dominate reach losses
- Smaller events can have higher loss ratio than larger events

Correspondence to:
M. S. Andersen,
m.andersen@unsw.edu.au

Citation:
McCallum, A. M., M. S. Andersen, G. C. Rau, J. R. Larsen, and R. Ian Acworth (2014), River-aquifer interactions in a semiarid environment investigated using point and reach measurements, *Water Resour. Res.*, *50*, 2815–2829, doi:10.1002/2012WR012922.

Received 9 SEP 2012
Accepted 26 FEB 2014
Accepted article online 2 MAR 2014
Published online 1 APR 2014

Abstract A critical hydrological process is the interaction between rivers and aquifers. However, accurately determining this interaction from one method alone is difficult. At a point, the water exchange in the riverbed can be determined using temperature variations over depth. Over the river reach, differential gauging can be used to determine averaged losses or gains. This study combines these two methods and applies them to a 34 km reach of a semiarid river in eastern Australia under highly transient conditions. It is found that high and low river flows translate into high and low riverbed Darcy fluxes, and that these are strongly losing during high flows, and only slightly losing or gaining for low flows. The spatial variability in riverbed Darcy fluxes may be explained by riverbed heterogeneity, with higher variability at greater spatial scales. Although the river-aquifer gradient is the main driver of riverbed Darcy flux at high flows, considerable uncertainty in both the flux magnitude and direction estimates were found during low flows. The reach-scale results demonstrate that high-flow events account for 64% of the reach loss (or 43% if overbank events are excluded) despite occurring only 11% of the time. By examining the relationship between total flow volume, river stage and duration for in-channel flows, we find the loss ratio (flow loss/total flow) can be greater for smaller flows than larger flows with similar duration. Implications of the study for the modeling and management of connected water resources are also discussed.

1. Introduction

A critical hydrological process is the interaction between rivers and aquifers [*Jones and Mulholland*, 2000]. Where groundwater levels are naturally or artificially lower than the riverbed, the flux of water from the river to the aquifer will be controlled by three factors: the differential head between river and aquifer, heterogeneity of the riverbed hydraulic conductivity, and whether an area of saturation can be maintained between the river and aquifer or whether decoupling will occur [*Desilets et al*., 2008; *Brunner et al*., 2009]. Since rivers experience large variations in flow in both space and time, and the hydraulic properties of the riverbed also vary, determining the river-aquifer interaction processes can be difficult from one field method alone. Moreover, many field measurements are often taken at one location and for short periods of time, therefore, the ability to extrapolate riverbed exchange over larger spatial and temporal scales is empirically constrained [e.g., *Kennedy et al*., 2008].

The interaction between rivers and aquifers can be measured at a point within the riverbed, inferred from hydraulic gradients, estimated from riverbed temperature profiles or using geochemical tracers, computed over a river reach from the water balance of surface flow, and from many other methods [e.g., *Cook*, 2012; *Anderson*, 2005; *Hatch et al*., 2006; *Constantz*, 2008; *Barlow et al*., 2000; *Harvey and Wagner*, 2000; *Ruehl et al*., 2006; *Rosenberry and LaBaugh*, 2008] (for a thorough review of many methods see *Kalbus et al*. [2006]). Generally, the field methods are of two types: those that attempt to measure the flux directly through the river-aquifer interface and those that measure volumetric flow changes along the river [*Becker et al*., 2004; *McCallum et al*., 2012a]. The first methodology provides estimates of the river-aquifer interactions at the point of measurement, while the second gives spatially averaged estimates. A combination of both approaches can therefore yield insights into the water exchange process operating within catchments. Despite the general theory of river-aquifer interactions being well developed [e.g., *Winter et al*., 1998], few field studies have

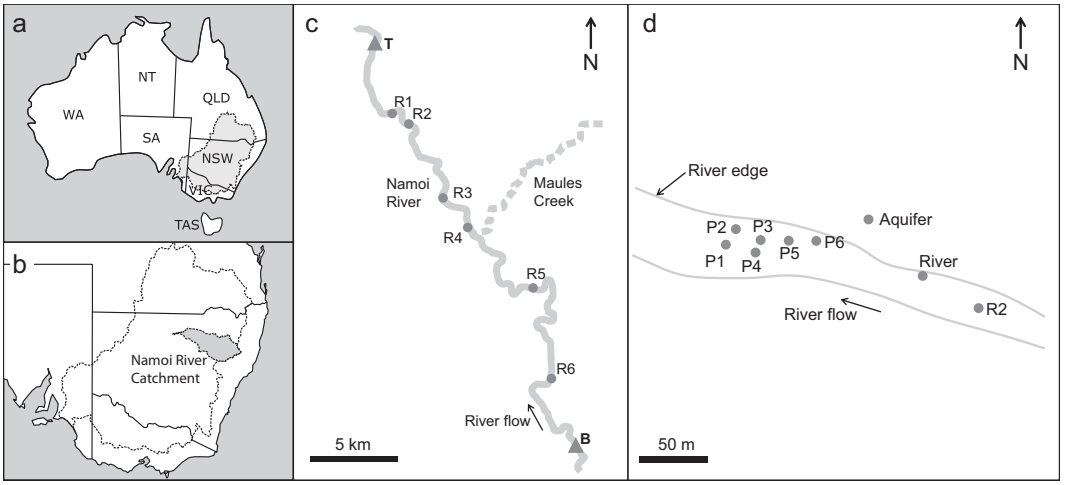

Figure 1. Location of (a) the Murray-Darling Basin in Australia and (b) the Namoi River Catchment. Temperature arrays (shown as circles) in two different deployments: (c) Reach (i.e., 1000s of meters) and (d) Pool (i.e., 10s of meters). Also shown are the river gauging stations (triangles).

measured both the spatial and temporal variation of water fluxes from multiple methods [e.g., *Su et al.*, 2004; *Constantz et al.*, 2003].

This study examines the river-aquifer flux characteristics along a 34 km reach of a low-gradient alluvial meandering river in semiarid eastern Australia. By measuring temporal changes in riverbed temperatures with depth, natural heat is used as a tracer to derive vertical Darcy fluxes at two spatial scales: high-density single pool deployment and evenly spaced reach deployment, over a range of flow conditions. On a larger scale, these results are complemented with an analysis of the water balance between two gauging stations over the entire 34 km reach in which the point measurements were made. Importantly, this allows for a qualitative assessment of the processes controlling the temporal variations in the reach water balance as well as river-aquifer interactions in general. This is intended to: (1) identify the processes controlling the variation in the timing and magnitude of riverbed Darcy fluxes and (2) compare the processes with the dynamics of the reach water balance as determined from differential gauging.

2. Study Area

The Murray-Darling Basin is Australia's largest river basin (Figure 1a), covering 14% of the continent's surface area, and generates about 40% of the national income derived from agricultural production. Within the basin, agricultural issues and sustainable water management are environmentally and politically sensitive [*MDBA*, 2010; *ABS*, 2012].

The Namoi River Catchment (Figure 1b) is a major subcatchment of the Murray-Darling Basin, with a surface area of about 42,000 km^2. The Namoi River is over 350 km long, and ranges in elevation from over 1500 m in its headwater tributaries in the east to 100 m in the west. It has one of the highest groundwater abstraction levels in Australia. Sharing of water between competing users, as well as the environment, has led to the establishment of rules as to how water can be used and traded in the catchment [*Burrell et al.*, 2011].

The study focuses on a 34 km reach of the Namoi River where it runs south to north through a semiarid tributary catchment, Maules Creek. The alluvial plains of the catchment are situated 200–250 m above sea level. To the north and east is the Nandewar Range, which has peaks rising to 1500 m. Below and to the east of the Namoi River is a 120 m deep palaeochannel filled with clay, sands, and gravels. Groundwater is abstracted for flood irrigation as well as for stock and domestic use. Some surface water is also diverted for irrigation purposes, although this volume is small and comprises only about 7% of the total irrigation usage [*Andersen and Acworth*, 2009]. Maules Creek is the main tributary, flowing from the mountains in the east, and is generally ephemeral although it does have perennial flow in its midreach [*Rau et al.*, 2010]. Due to its

intermittent nature, Maules Creek only contributes flow to the Namoi River during infrequent floods [*Andersen and Acworth*, 2009].

Groundwater recharges at the mountain front in the east of the catchment and in the past it discharged into the Namoi River in the west. However, due to groundwater abstraction, which started in the 1980s, the groundwater levels have been lowered such that the river reach has changed from being predominately gaining to predominantly losing during nonflood periods [*McCallum et al*., 2013].

Further background information about the catchment, including details of the hydrological and geological context, can be found in *Giambastiani et al*. [2012] and *McCallum et al*. [2013].

3. Methodology

3.1. Point Measurements From Temperature Time Series

3.1.1. Theory

The convection-conduction equation for one-dimensional fully saturated conditions can be formulated as

$$\frac{\partial T}{\partial t} = D\frac{\partial^2 T}{\partial z^2} - v\frac{\partial T}{\partial z}, \tag{1}$$

where T is temperature, t is time, z is depth, v is thermal front velocity, and D is effective thermal diffusivity [*Suzuki*, 1960].

For the situation of a semi-infinite half-space with a sinusoidally varying temperature at the upper surface, the dampening in recorded temperatures can be used to estimate the thermal front velocity by

$$-v = \frac{2D}{\Delta z}\ln(A_r) + \sqrt{\frac{\alpha + v^2}{2}}, \tag{2}$$

and

$$\alpha = \sqrt{v^4 + \left(\frac{8\pi D}{P}\right)^2}, \tag{3}$$

where A_r is amplitude ratio and P is period [*Hatch et al*., 2006].

The site-specific thermal diffusivity (for substitution into equations (2) and (3)) can be estimated using both the dampening and phase shift in the recorded temperatures, during nonflow event periods, with

$$D = \frac{\Delta z^2 P^2 \ln A_r \left(4\pi^2 \Delta\Phi^2 - P^2 \ln^2 A_r\right)}{\Delta\Phi\left(P^2 \ln^2 A_r + 4\pi^2 \Delta\Phi^2\right)\left(P^2 \ln^2 A_r - 4\pi^2 \Delta\Phi^2\right)}, \tag{4}$$

where $\Delta\Phi$ is the phase shift [*McCallum et al*., 2012a].

The thermal front velocity and Darcy flux are then related using

$$q = \gamma v, \tag{5}$$

and

$$\gamma = \frac{n\rho_w c_w + (1-n)\rho_s c_s}{\rho_w c_w}, \tag{6}$$

where q is Darcy flux (a negative value indicates losing conditions); n is porosity; ρ_w and c_w are the density and heat capacity of water; and ρ_s and c_s are the density and heat capacity of solids [*Buntebarth and Schopper*, 1998].

It is important to note that this method assumes: (1) the porous media is saturated with a single fluid, (2) fluid flow is in the vertical direction only, (3) fluid flow is in a steady state, (4) fluid and solid properties are constant in both space and time, and (5) fluid and solid temperatures at any particular point in space are equal at all times [*Stallman*, 1965].

3.1.2. Field Measurements

Two types of temperature array designs were used for field deployment. The first consisted of temperature sensors (Onset HOBO Pro v2) at 0.00, 0.15, and 0.30 m depth within a 32 mm diameter PVC pipe. The sensors were separated by insulating spacers. At each measuring depth the pipe was perforated to allow rapid thermal equilibrium. The second design consisted of pressure/temperature sensors (Solinst Levelogger Gold 3001) at 0.00 and 1.00 m depth and temperature sensors (Onset HOBO Pro v2) at 0.18 and 0.34 m depth. The other features remained the same as in the first design. The arrays were installed vertically into the riverbed and the locations were determined using Differential Global Positioning System (DGPS).

Temperature arrays were installed in the riverbed in two separate deployments: within a single pool and then evenly spaced along the 34 km reach. For each deployment, six arrays were installed (Figures 1c and 1d). It should be noted that the two deployments spanned different periods: the pool arrays were deployed from November 2007 to April 2008 (i.e., 164 days) and the reach arrays from October 2009 to December 2010 (i.e., 415 days). The pool is monitored for river stage and is adjacent to the site where the groundwater level is measured ($\sim$40 m from the river). All parameters were logged every 15 min.

3.1.3. Data Processing and Interpretation

The raw temperature time series were filtered (i.e., two-pass forward and backward bandwidth filtering using a Tukey window with all-pass frequencies of 0.9–1.1 cycles per day) to extract time series of temperature amplitudes and phases [see *Rau et al*., 2010]. Filtering ensures that the dominant daily sinusoid is correctly extracted from all other "environmental noise" contained in the temperature measurements. The data obtained from filtering complies with the method's requirement for a sinusoid and contains amplitudes and phases that are free from obfuscation [*Lautz*, 2012]. Two pairs of temperature time series were used from each array: the upper and second sensors and the second and third sensors. From these, the temperature amplitude ratios and phase shifts were calculated, and then used to create a time series of Darcy flux (q) for each array using equations (2–6).

Basic statistics (i.e., minimum, maximum, average, standard deviation) were computed for all point measurements separately for both low flows and high flows. The threshold between low flow and high flow for all analyses within this paper is defined 1.5 GL/d (n.b. GL is Giga liter, i.e., 1 GL $= 1 \times 10^6$ m^3), based on a previous analysis of flow duration curves [see *McCallum et al*., 2013].

The correlation between the riverbed Darcy fluxes obtained from the first and second and that from the second and third temperature logger was calculated for each array to check if the 1-D vertical flow assumption is valid. The correlation between the river stage and the riverbed Darcy flux was also computed for each array, to determine the degree to which variation in river stage drives the changes in the riverbed Darcy flux.

3.2. Reach Measurements From Differential Gauging

Gauging stations are located at the upstream (Boggabri) and downstream (Turrawan) ends of the reach separated by 34 km (Figure 1c). These stations record the river stage each hour which is then postprocessed to give flow using a calibrated rating curve [*DNR*, 2011]. Hourly data for a 5 year period (2007–2012 water years; October to September) were used. This data set covers the period of the temperature array deployments, and also overlaps with that presented in *McCallum et al*. [2014] (i.e., water years 2000–2010).

For both gauging stations, the cumulative flows, cumulative within-channel flows (defined as $<$25 GL/d), and cumulative low flows (defined as $<$1.5 GL/d) were computed. The losses (GL) and time (% of total time) for these different flow regimes were also computed.

Each flow event within this 5 year period was then extracted and analyzed using the method of *McCallum et al*. [2014]. In this method, the hydrographs recorded at the upstream and downstream ends of a river reach are used to estimate the loss volume for a flow event, as well as the loss rate during the event.

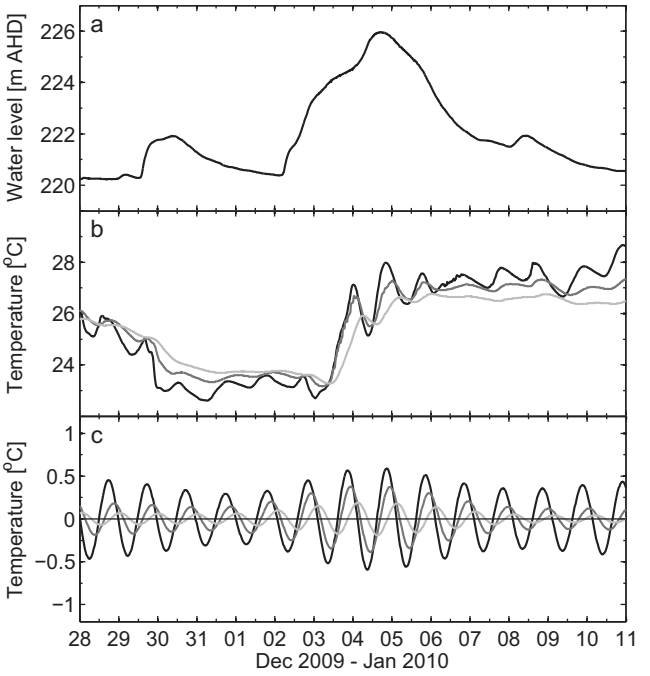

Figure 2. (a) River hydrograph for 14 days. (b) Unprocessed temperature data from temperature array P1 for depths 0, 15, and 30 cm, same period. (c) Temperature data filtered for frequencies of 0.9–1.1 cycles per day using bandwidth filtering.

The starting point of the method is the water balance for a river reach:

$$Q_u + Q_i + Q_f = Q_d + Q_o + E_a + \frac{\Delta S}{\Delta t}, \quad (7)$$

where Q_u is flow at the upstream end of the reach, Q_i is flow into the reach (e.g., tributaries), Q_f is river-aquifer flux, Q_d is flow at the downstream end of the reach, Q_o is flow out of the reach (e.g., surface water diversions), E_a is evapotranspiration from the reach, and $\frac{\Delta S}{\Delta t}$ is the change in channel storage with time. All components of the water balance have dimensions (L^3/T).

For the specific case when flow into and out of the reach, as well as evapotranspiration, are small compared to the magnitude of flow at the upstream and downstream ends of the reach, the loss volume (LV) can be computed by:

$$LV = \sum Q_d - \sum Q_u, \quad (8)$$

and the loss ratio (LR; flow loss/total flow) can be computed by:

$$LR = \frac{\sum Q_u - \sum Q_d}{\sum Q_u}. \quad (9)$$

By introducing the concepts of time-shifted upstream and downstream hydrographs (for details, see *McCallum et al*. [2014]), the loss rate (LRt) at any point in time during an event can then be estimated using:

$$LRt = Q_d^t - Q_u^t. \quad (10)$$

The applicability of these three equations to field data depends on whether the assumption is reasonable that other loss/gain mechanisms (e.g., evapotranspiration, inflows) are minimal. This is considered in further detail in the discussion below.

For these calculations, the time intervals are equal for each component in the original water balance, and the integration is over the event duration. The start/end time for each flow event was defined as the time corresponding to the lowest flow at the upstream gauge in the 7 days prior to/following a recorded flow of 1.5 GL/d. For the loss volume (LV) and loss rate (LRt), a negative value indicates a loss from the river, and a positive value indicates a gain to the river.

For each flow event, the event duration, maximum upstream stage and flow, loss volume (i.e., using equation (8)), maximum and average loss rates (i.e., using equation (9)), and loss ratio (i.e., using equation (10)) were calculated.

4. Results

4.1. Point Measurements From Temperature Time Series

A representative 14 day period of temperature data collected during a flood event (Figure 2a) is shown in Figure 2. The measured temperature time series shows strong diel heat patterns as well as longer-term heat trends caused by changes in the weather (i.e., storm) and noise (Figure 2b). The filtered time series more clearly reveals the dampening of amplitude and shift in phase with depth at each location (Figure 2c).

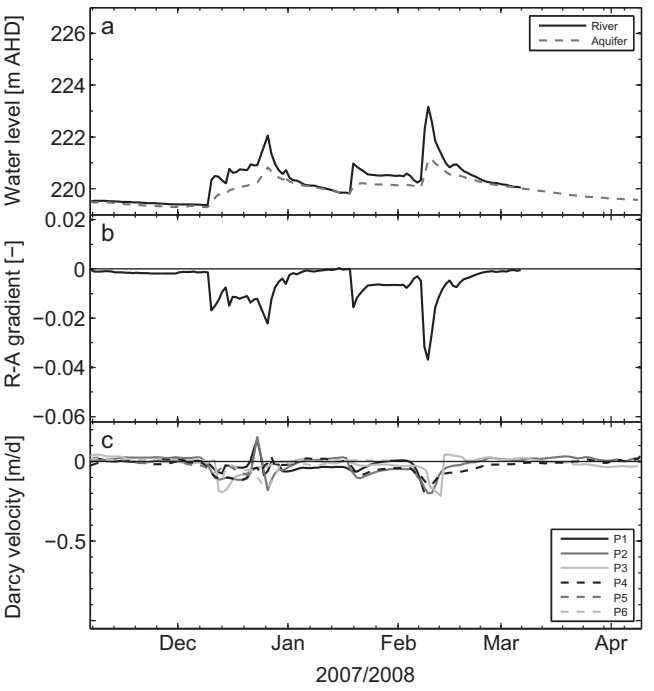

Figure 3. Results for the pool deployment. (a) River and aquifer hydrographs. (b) River-aquifer (R-A) gradient (negative value indicates potentially losing conditions). (c) Estimated Darcy fluxes from riverbed temperature data.

During the monitoring of riverbed temperatures in the pool four main flow events were recorded (Figure 3). Two of these were large (∼3–4 m stage increase) events caused by rainfall-derived runoff and two were smaller (∼1 m stage increase) events caused by upstream dam releases, which preceded each of the rainfall events. The groundwater levels responded in a damped fashion to each of the flow events (Figure 3a, dashed line). The corresponding times series of the river-aquifer gradient was close to zero or slightly negative (toward the aquifer) during low flows, but becomes distinctively negative (hydraulic gradients of −0.01 to −0.04) during the high flows (Figure 3b).

During low flows, the temperature data for all arrays in the pool gave Darcy flux results that indicated approximately neutral conditions (∼0.0 m/d), while during high flows they showed losing conditions (up to ∼−0.3 m/d; Figure 3c and Table 1). In some cases, slightly gaining conditions (∼0.1 m/d) were observed following flow events. Over depth, the correlation between fluxes estimated from probes 1 and 2 (v_{1-2}) and probes 2 and 3 (v_{2-3}) was significant ($r > 0.65$) at three locations within the pool (i.e., arrays P2, P4, and P6; Table 1). At these same locations, the correlation between stage and flux was also significant (Table 1).

Two main flow events were recorded during the reach monitoring period (Figure 4a, solid line). One was a large event caused by rainfall (∼6 m stage increase) and the other was a smaller event caused by a dam release (∼1 m stage increase), which preceded the rainfall event. As for the pool data, the groundwater

Table 1. River-Aquifer Statistics (See Figures 3 and 4)[a]

	Low Flows					High Flows					All flows			
Array	Data (-)	Minimum (m/d)	Maximum (m/d)	Average (μ) (m/d)	Standard Deviation (σ) (m/d)	Data (-)	Minimum (m/d)	Maximum (m/d)	Average (μ) (m/d)	Standard Deviation (σ) (m/d)	Data (-)	Cor. 1 (-)	Data (-)	Cor. 2 (-)
Pool Data														
P1	50	−0.07	0.02	−0.01	0.03	45	−0.25	0.18	−0.04	0.06	150	0.14	95	−0.43
P2	58	−0.13	0.04	0.02	0.03	62	−0.26	0.20	−0.08	0.08	93	**0.73**	120	**−0.76**
P3	58	−0.23	0.06	0.00	0.04	56	−0.28	0.06	−0.04	0.07	115	0.33	114	−0.41
P4	57	−0.13	0.03	−0.01	0.02	65	−0.19	0.04	−0.08	0.05	141	**0.84**	122	**−0.65**
P5	35	−0.06	0.03	0.00	0.02	12	−0.11	0.07	−0.06	0.05	44	0.54	47	−0.62
P6	43	−0.04	0.02	0.01	0.02	25	−0.21	0.01	−0.07	0.07	37	**0.97**	68	**−0.86**
Reach Data														
R1	233	−0.58	0.09	−0.05	0.07	31	−0.58	0.07	−0.17	0.13	264	0.31	264	−0.57
R2	201	−0.07	0.09	0.01	0.02	61	−0.84	0.31	−0.10	0.23	262	**0.79**	262	**−0.66**
R3	32	−0.09	−0.02	−0.05	0.02	23	−0.15	−0.02	−0.08	0.04	55	**0.68**	55	−0.42
R4	34	−0.15	0.02	−0.06	0.05	24	−0.58	0.01	−0.34	0.16	58	**0.81**	58	**−0.80**
R5	195	−0.99	−0.13	−0.23	0.13	46	−1.20	−0.17	−0.54	0.26	12	**0.92**	241	−0.52
R6	207	−0.27	0.04	−0.05	0.03	53	−0.55	−0.05	−0.18	0.14	257	**0.95**	260	**−0.78**

[a]"Cor. 1" refers to correlations between v_{1-2} and v_{2-3} and "Cor. 2" refers to correlations between stage and flux (v_{1-2}). Bold indicates |Correlation coefficient| ≥ 0.65.

Table 2. Analysis of High-Flow Events From Upstream and Downstream Gauging Stations (See Figures 6 and 7)[a]

Event Number	Event Start Date	Duration (Days)	Maximum River Stage (m)	Maximum River Flow (GL/d)	LV (GL)	LR (%)	Maximum LRt (GL/d)	Average LRt (GL/d)
1	10/12/06	16	1.5	2.1	−6.2	29	−0.6	−0.4
2	24/12/06	13	1.3	1.8	−4.2	23	−0.4	−0.3
3	30/12/06	6	1.2	1.6	−1.4	20	−0.3	−0.2
4	4/3/07	13	3.0	6.5	−2.0	26	−1.6	−0.2
5	13/6/07	14	3.6	8.7	−2.8	18	−1.6	−0.2
6	27/12/07	14	4.4	12.4	−4.0	17	−2.0	−0.3
7	13/2/08	14	4.0	10.5	−3.3	9	−0.9	−0.2
8	2/12/08	20	7.1	49.1	−29.1	22	−10.3	−1.5
9	19/12/08	15	6.4	26.4	−10.9	13	−3.3	−0.8
10	16/12/09	8	1.4	1.8	−2.4	22	−0.4	−0.3
11	24/12/09	8	1.3	1.6	−1.0	12	−0.2	−0.1
12	30/12/09	4	2.5	4.7	0.6	−8	0.0	0.1
13	18/1/10	8	1.8	2.8	−0.9	14	−0.4	−0.1
14	19/7/10	14	2.8	5.6	−2.4	16	−0.8	−0.2
15	18/8/10	38	6.5	28.1	−18.1	8	−2.2	−0.5
16	5/9/10	1	1.3	1.5	−0.2	20	−0.3	−0.3
17	21/10/10	6	1.6	2.4	−3.5	48	−1.1	−0.6
18	29/10/10	10	1.5	2.0	−5.3	46	−0.9	−0.6
19	29/10/10	11	1.5	2.0	−5.8	46	−0.9	−0.5
20	20/11/10	19	5.3	16.8	−32.8	27	−3.3	−1.8
21	28/12/10	57	7.6	79.4	−81.4	11	−7.2	−1.4
22	3/2/11	11	1.4	1.9	−2.9	17	−0.3	−0.3
23	10/2/11	4	1.3	1.6	−0.8	15	−0.2	−0.2
24	14/2/11	12	1.4	1.7	−1.9	13	−0.2	−0.2
25	25/6/11	17	2.4	4.4	−4.1	13	−0.6	−0.3
26	14/9/11	14	1.4	1.7	−2.2	16	−0.3	−0.2

[a]Note: GL is Giga liter, i.e., 1 GL = 1×10^6 m^3.

levels responded in a damped fashion to each of the flow events (Figure 4a, dashed line). The corresponding river-aquifer gradient in Figure 4b shows losing conditions during the high flood period with hydraulic gradients varying from −0.02 to −0.06. Following the flow events, gaining conditions with hydraulic gradients up to 0.01 were observed to last for a period of almost 3 months.

During low flows, the Darcy fluxes from the reach data indicated neutral to slightly losing conditions (+0.05 to −0.10 m/d) with the exception of array R5 which showed overall losing conditions (approximately −0.15 m/d; Figure 4c and Table 1). During high flows, the Darcy fluxes showed losing conditions (up to −1.20 m/d; Figure 4c and Table 1). Immediately after the high-flow event, there were gaining conditions (>0.10 m/d) at array R2 which diminished over one and a half weeks to neutral conditions (Figure 4c). The correlation between v_{1-2} and v_{2-3} was greater than 0.65 at all locations along the reach except for one (array R1; Table 1). At three locations, the correlation between river stage and flux was greater than 0.65 (i.e., arrays R2, R4, and R6; Table 1).

4.2. Reach Measurements From Differential Gauging

The hydrographs for Boggabri and Turrawan (Figure 5a; black and gray lines) show that river flows are episodic and vary from 0 to 79 GL/d for the 5 year period analyzed. The cumulative hydrographs show that 2031 GL entered the catchment while 1719 GL left the catchment over the 5 year period, which corresponds to a loss of 311 GL (Figure 5b; solid lines). If the overbank events are excluded from this analysis, then these statistics change to 1758 GL entering, 1558 GL leaving, and a lower total loss of 199 GL (Figure 5b; dashed lines). When only low flows are considered (Figure 5c), the corresponding statistics are 711, 589, and 113 GL, respectively (Figure5).

The losses during low flows (which occur 89% of the time) account for 36% of all losses (i.e., 113/311), or alternatively 57% of losses (i.e., 113/199) when overbank events are excluded. The losses during high flows (which occur 11% of the time) account for 64% of all losses, or alternatively 43% when overbank events are excluded.

For the 5 year period, high-flow events (i.e., flows greater than 1.5 GL/d) were analyzed (Table 2 and Figures 6 and 7). The duration of these events varied from 1 to 57 days, maximum stage from 1.2 to 7.6 m,

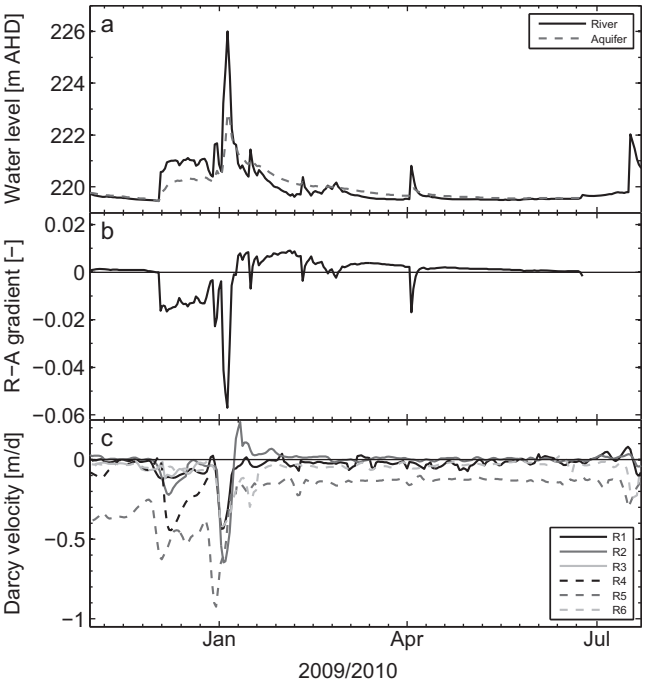

Figure 4. Results for the reach deployment. (a) River and aquifer hydrographs. (b) River-aquifer (R-A) gradient (negative value indicates potentially losing conditions). (c) Estimated Darcy fluxes from riverbed temperature data.

maximum river flow from 1.2 to 76.1 GL/d, loss volume per event from −0.2 to −81.4 GL, maximum loss rate from −0.2 to −10.4 GL/d, average loss rate from −0.1 to −1.7 GL/d, and loss ratios from 8 to 48%. Excluded from these reported ranges is one event which had a positive reach loss result (i.e., a gain of water to the river; see event 12 in Table 2). It is unlikely this gain is due to surface flow contributions from Maules Creek as the flow event was of comparatively short duration and magnitude. With the available data, it is not possible to determine the reason for this outlier.

5. Discussion

5.1. Limitations of Point and Reach Measurements

This study uses two different methods to investigate river-aquifer interactions in a semiarid environment. In the sections that follow, the structure of the Methodology and Results is not repeated, where first the point measurements were considered and then the reach measurements, but rather various processes are discussed, drawing on the different measurements as required. In this connection, it is also important to note that neither method directly measures the water volumes exchanged between the river and the aquifer. Rather, whether used independently or together, they provide useful information on the hydrological processes occurring at different spatial and temporal scales [*Scanlon et al.*, 2002; *Kalbus et al.*, 2006]. Before drawing conclusions from the results, the advantages and limitations of each method are first considered.

While the use of heat as a tracer of water movement through riverbeds has increasingly become popular over the last decade [*Constantz*, 2008], a number of authors have highlighted the strengths and potential problems of the method when applied to field data. These problems arise primarily from the potential for field conditions to differ from the idealized 1-D assumptions, and could be due to nonvertical flow fields [e.g., *Lautz*, 2010; *Roshan et al.*, 2012; *Cuthbert and Mackay*, 2013], the presence of gas in organic-rich streambeds [e.g., *Cuthbert et al.*, 2010], hydraulic heterogeneity in the riverbed introducing horizontal temperature gradients [*Schornberg et al.*, 2010; *Ferguson and Bense*, 2011; *Rau et al.*, 2012b], and uncertainty in the thermal parameters [*Shanafield et al.*, 2011; *Soto-López et al.*, 2011]. Finally, the heat tracing method only measures fluxes in the shallow streambed and may not accurately distinguish between hyporheic and more regional groundwater exchange [e.g., *Bhaskar et al.*, 2012]. However, heat tracing using temperature time series has been comprehensively tested in the laboratory, which demonstrates that the flux estimates are robust and reliable when the inherent assumptions are valid [*Rau et al.*, 2012b], even during transient conditions [e.g., *Lautz*, 2012]. In the context of this study, the fluxes derived from heat tracing at discrete points within the river are largely indicative of vertical streambed flow activity and therefore potential stream-aquifer exchange, with some uncertainties discussed in section 5.5.

The application of the differential field gauging method also contains important limitations. The most fundamental is whether the river reach water balance can be simplified to a single input and output. Flow contribution from smaller tributaries, flow abstraction by surface water pumps, and evapotranspiration all impact on the results [*Lerner et al.*, 1990]. Based on a previous catchment water balance study of the studied catchment, this is a reasonable simplification to make for the present study [*Andersen and*

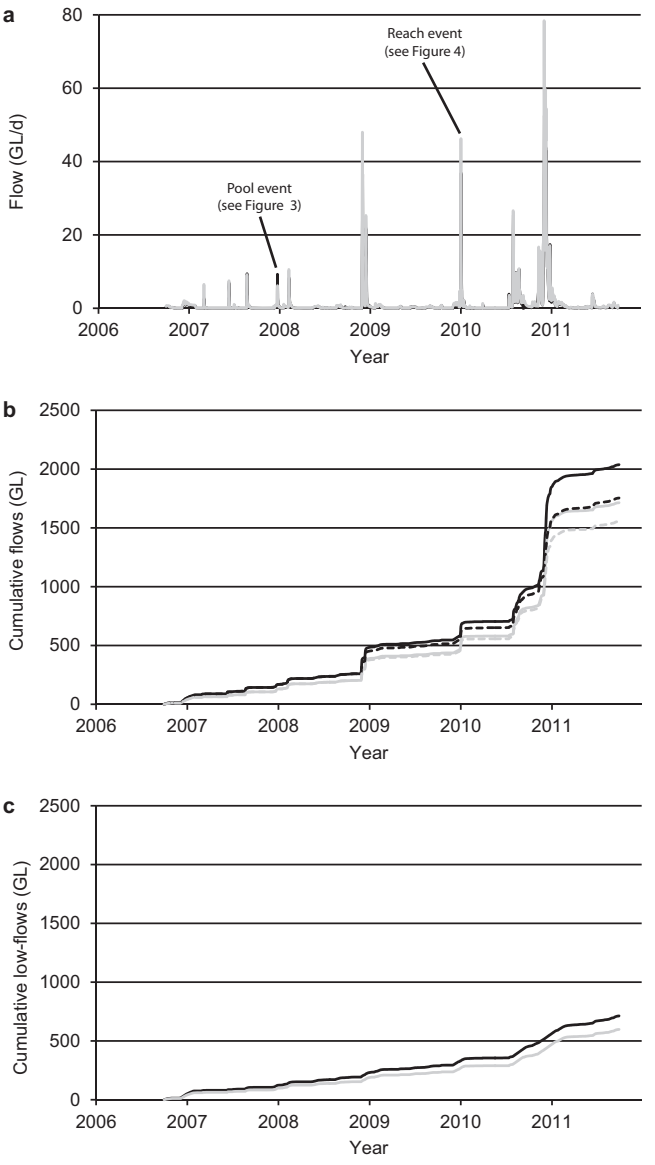

Figure 5. (a) River hydrographs. (b) Cumulative hydrographs for upstream and downstreams flows for analysis including overbank events (solid lines) and excluding overbank events (dashed lines). (c) Cumulative hydrographs for low flows. In Figures 5a–5c, the black line is upstream flow (at Boggabri) and gray line is downstream flow (at Turrawan). Note: GL is Giga liter, i.e., 1 GL = 1×10^6 m^3.

Acworth, 2009]. Further issues may arise because the method is not sensitive to small-scale processes and instead provides an averaged value for the interactions over the whole reach, which may differ from point measurements [*de Vries and Simmers*, 2002]. Thus, small-scale losses and gains may occur simultaneously with the context of a larger reach-scale net loss or gain [*McCallum et al*., 2012b]. Also, when interpreting the differential gauging data, it should be noted that the concept of river-aquifer interactions itself may be too simplistic [*McCallum et al*., 2014]. Water "lost" from the river may return to the river but on spatial and temporal scales large and long enough to not be considered "return flow" or "bank storage." Finally, gauging data itself will always contain inaccuracies, especially at very low- and very high flows [*McCallum et al*., 2014]. Despite the inherent uncertainties in gauging data, the data for the two gauges utilized are overall reliable, and the big picture of the interactions gained remains robust [*Tomkins*, 2014].

5.2. River Flow Events and River-Aquifer Interactions

All the point measurements of Darcy fluxes within the riverbed show similar responses to flow events, however, they have divergent responses during recession and low flows (Figures 3c and 4c and Table 1). During low-flow conditions, the point-scale measurements indicate slightly gaining to slightly losing fluxes. During a flow event, however, these fluxes uniformly respond by becoming higher magnitude losses. During flow recession, one point measurement (R5) indicates an immediate reversal to gaining conditions (in both riverbed Darcy flux and gradient data), while the rest of the measurements return to a low slightly gaining to slightly losing Darcy flux.

The most obvious explanation for the temporal variability of riverbed Darcy fluxes and their magnitude is the simultaneous variation in river stage, which drives the change in hydraulic gradient throughout the reach (Figures 3 and 4). Given the smaller variation in the groundwater level over time, it is clear that the dynamic variation of river height, particularly the flood wave, is the primary driver of changes in the Darcy flux through the riverbed. The temporal match between the change in hydraulic gradient and the independent measurements of riverbed Darcy fluxes gives confidence in the temperature-based results.

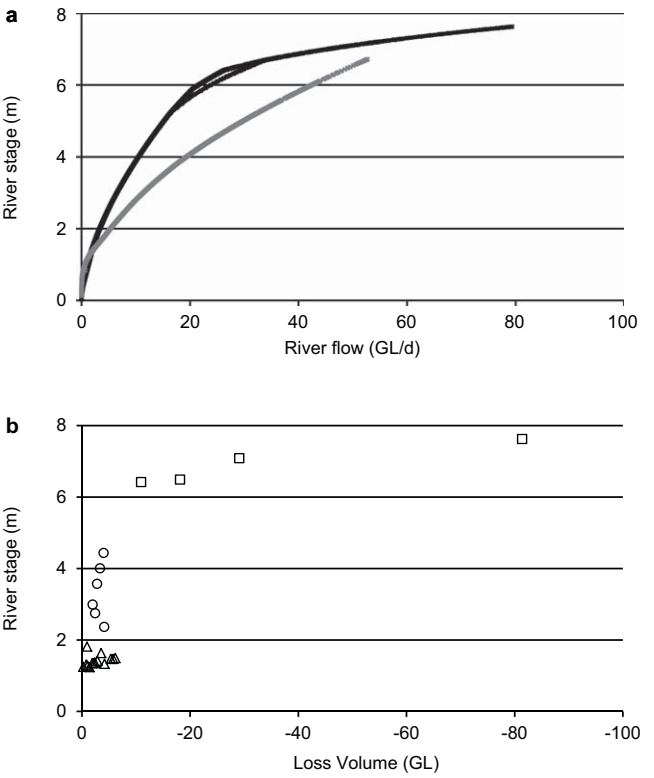

Figure 6. For all high-flow events (i.e., flows larger than 1.5 GL/d) for the 5 year period analyzed, (a) the observed relationship between river stage and river flow for upstream (black crosses) and downstream (gray crosses) gauging stations; (b) the observed relationship between river stage and reach loss. For Figure 6b, the triangles represent events with peak flows less than 4 GL/d, the circles represents between 4 and 25 GL/d, and the squares represents more than 25 GL/d (i.e., overbank flows). Note: GL is Giga liter, i.e., 1 GL = 1×10^6 m^3.

These point-scale observations of the significance of river flows on the interactions are complemented by an analysis of the differential river gauging data for the river reach (Figure 5). Under high flow conditions, which have occurred only 11% of the time in the 5 year record examined here, losses through the riverbed account for 64% (or 43% if overbank events are excluded) of all losses in the reach water balance. This supports the point-scale results in highlighting the important role of high-flow events in the interactions between rivers and shallow alluvial aquifers in semiarid and arid systems, a finding similar to that of previous studies [e.g., *Shentsis et al*., 1999; *Dahan et al*., 2007].

5.3. Overbank Flow Events and Potential Recharge

Additional insight into the influence of river flows on river-aquifer interactions is gained by further analysis of the flow events (Table 2 and Figures 6). Through rainfall-runoff processes and dam releases, the Namoi River experiences a wide range of flow magnitudes, with a resulting stage range of almost 8 m at the upstream gauge. For the 5 year period analyzed, <1% of flows were overbank at the upstream gauge, while none were overbank at the downstream gauge as a result of the increased bankfull capacity (>50 GL/d; i.e., water must reenter the channel along the reach). The low frequency of overbank flows, however, does not diminish their significance for the reach water balance. Rather, overbank events generate the largest reach loss volumes (between 10 and 80 GL per event) of all the examined flow events. This is intuitive since under these conditions a much larger part of the landscape (i.e., surface area) is included in overbank flows. In contrast, the largest within-channel event has a reach loss volume of only 6.2 GL. Thus, very infrequent overbank reach losses can be a significant source of potential recharge to the shallow aquifers for this section of the Namoi River.

It must be noted that these estimates of loss from the differential gauging represent maximum possible values of aquifer recharge (i.e., potential recharge). Evaporation from stagnant water on the floodplain, as well as evapotranspiration of floodwaters stored in the soil, will reduce the amount of water that eventually will become a flux of water from river to aquifer (i.e., actual recharge). Furthermore, a thin veneer of sediments across the floodplain can be of critical importance in controlling the amount of recharge [*Doble et al*., 2012]. However, given the remote location of this study site there is no data available to estimate evaporation surfaces or plant available soil moisture, and little work has been done in the area on the significance of overbank flow as a recharge mechanism [see *Jolly et al*., 1994]. Thus, in order to understand the true significance of overbank flow events for the river-aquifer interactions, further investigation of the evaporative and soil moisture storage processes is required.

Given that the overbank flow events can skew the interpretation of the loss estimates due to the complication of additional flow processes, it is instructive to exclude them from the water balance analysis. When this is done, the losses during within-channel high flows (which occur only 11% of the time) decrease from

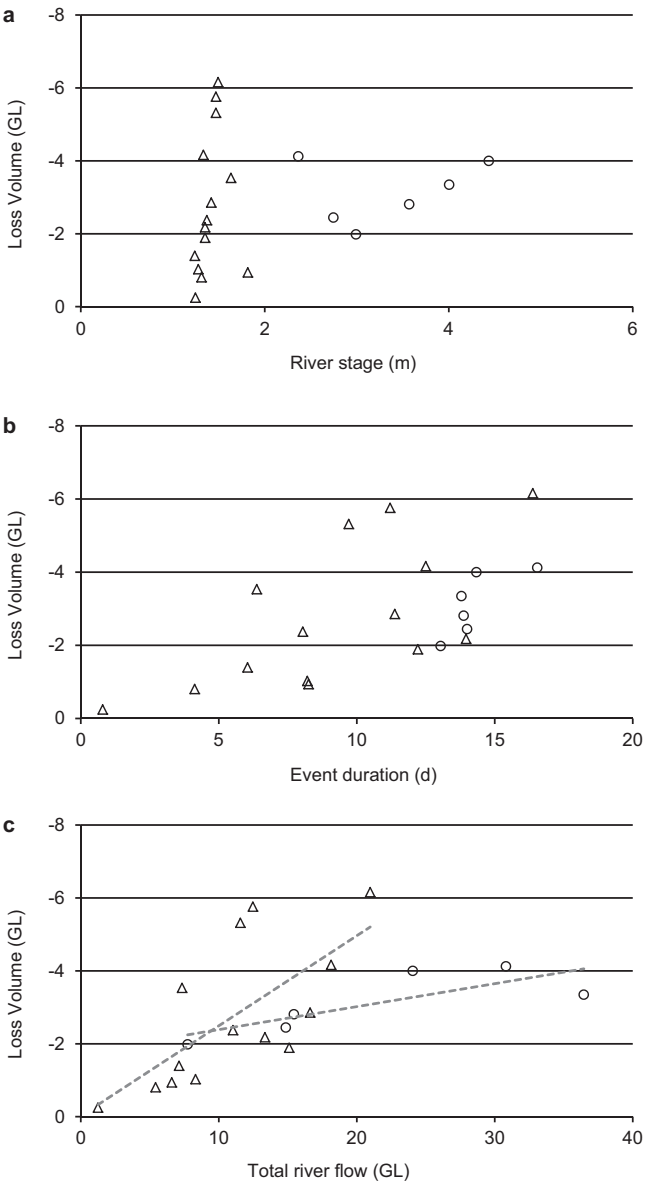

Figure 7. Dependence of reach loss for within-channel high-flow events (i.e., flows larger than 1.5 GL/d but less than 25 GL/d), on (a) river stage, (b) event duration, and (c) total river flow. In all figures, the triangles represent events with peak flows less than 4 GL/d and the circles represents more than 4 GL/d. Note: GL is Giga liter, i.e., 1 GL = 1×10^6 m^3.

64% of all losses to 43%. Despite this reduction, the percentage of losses accounted for by high-flow within-channel events is still very high compared to their frequency, and therefore the general conclusion of the significance of the high-flow events for the river-aquifer interactions is maintained.

5.4. In-Channel Flow Events and River-Aquifer Interactions

When focusing on the within-channel flows (Table 2 and Figure 7a), the relationship between the total reach losses and the river stage is surprisingly weak. Thus, while an increase in stage potentially leads to increased reach losses, the point-scale temperature data (Figures 3 and 4) demonstrate that additional factors must also be controlling these losses. Further scrutiny of Figure 7a shows that the data fall into two groups: one with low river stages (i.e., 1.2–1.8 m) but with a large range in loss volumes (0.2–6.2 GL; the triangles in Figure 7a), and another with larger river stages (i.e., 2.4–4.4 m) but without proportionally larger loss volumes (3–4.1 GL; the circles in Figure 7a). As some events with smaller stages clearly lead to greater loss volumes, one explanation might be that these events are also longer in duration, allowing more time for the loss to occur. However, this is not the case, since low-stage high-loss events (triangles) have a similar duration to the high-stage events with moderate loss (the circles Figure 7b). Therefore, the loss ratio is clearly different as events proceed beyond the 2 m stage range, suggesting other factors may be responsible.

These two groups based on stage range also remain apparent when reach loss is considered as a function of total river flow (Figure 7c). The ratio of the reach loss to cumulative flow (i.e., total river flow) is also indicative of the loss ratio, with the slope of the trends representing the overall loss ratio for these two groups. For the smaller events (i.e., the triangles, which have stages $<\sim$2 m), this ratio is $\sim$25%, much higher than the 6% for the larger events (i.e., the circles, which have stages $>\sim$2 m; see loss ratio results for individual events in Table 2).

One plausible explanation for the importance of river stage in determining reach losses is that the hydraulics of the system changes as the stage rises between the different magnitude flow events. That is, as the river stage increases, there is proportionally more water flowing within the channel due to increased

hydraulic efficiency, than is lost from the river. The response of the aquifer heads to the river flow, and the ability of the aquifer to transmit away any water lost from the river as the event progresses will also be important in controlling overall losses from the reach. However, as detailed piezometric data are unavailable in this river reach, the extent of this influence is not possible to determine here.

Another possible explanation is that the hydraulic conductivity of the riverbed is higher than that within the upper banks, and that the riverbed in this case is a more direct route of loss than the riverbanks. This is supported by field observations that the upper banks are generally of clayey or loamy texture along the reach. Further investigation of the channel geometry, aquifer hydraulic heads, as well as the hydraulic conductivity distribution of the river system is required to determine which explanation accounts for the patterns in reach losses observed.

5.5. Role of Riverbed Sediment Heterogeneity and Hyporheic Flow

Compared to the reach scale, considerable heterogeneity in riverbed fluxes should be expected at the point scale [*Buffington and Tonina*, 2009; *Fleckenstein et al*., 2006; *Genereux et al*., 2008]. Indeed, the heat tracing data indicates significant spatial variability in vertical Darcy fluxes, both within and between the pool and reach data (see values of μ and σ in Table 1). This is consistent with recent findings that there is a large spatial variability in riverbed fluxes at the reach and even at the meter scale [*Lautz and Ribaudo*, 2012; *Angermann et al*., 2012]. Point-scale Darcy fluxes are similar during low-flow periods and become increasingly divergent during higher flow conditions. This divergence in flux is further amplified as the distance between arrays increases: i.e., the widely spaced reach measurements show much greater variation in peak Darcy fluxes than those within the pool.

There are at least two possible explanations for the variability in Darcy flux for identical river stage fluctuations. First, a variable distribution in riverbed hydraulic conductivity due to the natural variability in riverbed sediments will lead to a spatial variation in vertical fluxes. This heterogeneity in hydraulic conductivity is a well-documented phenomenon of riverbeds [e.g., *Storey et al*., 2003; *Cardenas et al*., 2004; *Buffington and Tonina*, 2009]. Second, departures from the 1-D flow field will also lead to spatially variable fluxes. Topographic features (e.g., ripples, bars, meanders) influence flow fields, drive hyporheic exchange, and thus have an effect on the subsurface heat flow [e.g., *Cardenas and Wilson*, 2007; *Roshan et al*., 2012; *Cuthbert and Mackay*, 2013]. Significant hyporheic exchange would therefore affect the estimates of the Darcy flux depending on the probe locations within the actual 3-D flow field [*Angermann et al*., 2012]. *Hyun et al*. [2011] found that point and area-averaged estimates of flux differed from each other and hypothesized that hyporheic exchange was occurring within the regional river-aquifer interactions. In a separate study, *Ward et al*. [2012] found that local in-river hydraulic gradients did not necessarily reflect the regional gradients. Thus, the cause of this spatial heterogeneity in fluxes for low-flow conditions cannot be known with certainty based on the temperature data alone. Under strongly losing or gaining conditions, however, hyporheic exchange is expected to have a diminished effect on the more regional flow field [*Cardenas*, 2009]. Therefore, hyporheic fluxes are more likely to contribute greater uncertainty to the flux estimates under low-flow conditions than during high flows, and the observed variability during high flows can be largely attributed to the effects of riverbed heterogeneity.

Assuming that the variability in Darcy fluxes observed at the pool scale is representative for other pools along the reach, this uncertainty can be propagated to all reach results under low-flow conditions. This allows the estimation of 10th and 90th percentiles (i.e., $\mu \pm 1.24\ \sigma$) for the Darcy fluxes, thereby giving a realistic uncertainty range to the reach results, without minimizing the complications of the heterogeneity and hyporheic exchange. Furthermore, this approach provides some guidance as to whether the estimated fluxes at each reach location are actually losing or gaining, or are simply the result of localized (hyporheic) fluxes.

Adding this uncertainty range to the results shows that the point measurement fluxes during low-flow conditions are comparable to a reach averaged low-flow estimate from the differential gauging. The Darcy fluxes derived from the temperature time series along the reach are neutral to slightly losing, with average 10th and 90th percentile values of -0.10 and -0.04 m/d. Taking the reach loss during low flows for the analyzed period, and by using an estimated reach length of 34 km and width of 20 m, the reach-scale 5 year average river-aquifer Darcy flux was estimated at -0.09 m/d. This compares favorably, though not

exactly, with the results from the temperature time series. The combination of both methods therefore confirms the reach is slightly losing overall during low-flow periods.

During high-flow events the divergence between point measurements can be large (Table 1). This suggests differing degrees of river-aquifer connectivity along the reach. Other researchers have found that flow through higher conductivity "windows" in semiarid and arid riverbeds is a significant pathway of water loss [e.g., *Shentsis and Rosenthal*, 2003]. The increased importance of these local exchanges under large hydraulic gradients must therefore be considered when accounting for the volume of river-aquifer interactions.

In addition to the spatial variability in riverbed sediments and hydraulic conductivity, there are two additional pieces of evidence to suggest that these also vary over time. First, in the case of array R3, the bed scour during the event was sufficient to remove the riverbed installation, and second, in the case of array R4, the same event caused deposition of sediment leaving the array buried within the riverbed to such a depth that the temperature sensors were no longer sensitive to diel variations. That riverbed scouring and deposition was occurring was confirmed during the removal of the temperature arrays. The effect of this sediment transport on hydraulic conductivity over time is difficult to quantify directly, however there are a small but growing number of field studies which have attempted to measured the temporal variability in riverbed hydraulic conductivity [e.g., *Springer et al*., 1999; *Genereux et al*., 2008; *Rau et al*., 2010; *Mutiti and Levy*, 2010; *Hatch et al*., 2010].

5.6. Implications for Numerical Modeling and Resource Management

Based on surface water hydrograph analysis, river aquifer gradients and modeling of the reach water balance, previous studies [i.e., *Giambastiani et al*., 2012; *McCallum et al*., 2013] suggested that the Namoi River should have become overall losing in recent years due to significant groundwater abstraction. The present results support the suggestion that the river is indeed losing at low flows by the direct measurements of the Darcy flow in the riverbed.

The large variability in vertical riverbed fluxes observed at different locations, and over time, raises questions as to the validity of inferring large-scale processes from point measurements. Whilst this variation is small during low-flow conditions, even within 10s of meters within the pool the results spanned gaining, neutral and losing conditions. Based on this finding, it would not be justifiable for the purpose of catchment-scale water exchange calculations to classify the river-aquifer interaction based on the temperature time series from a single array. However, provided variation at small spatial distances is first acknowledged and sufficiently understood, it may be possible to link point measurements of river-aquifer exchange to volumetric reach estimates for the low-flow conditions as done for this study. On the other hand, during high-flow events the volumes of interactions are not uniformly spread over the reach, which is consistent with interactions occurring predominantly through higher connectivity "windows" along the reach. Thus, upscaling point measurements without a sufficient understanding of these processes or spatial coverage of the reach will result in potentially erroneous estimations of the reach water balance under transient conditions. This conclusion is consistent with previous studies which highlight the challenges associated with upscaling point results to the reach and catchment scales under less transient conditions and for shorter time periods [*Lautz and Ribaudo*, 2012; *Angermann et al*., 2012].

A final implication of this study is that generalizations made in numerical models concerning the river-aquifer interactions, such as assuming a spatially and temporally invariant conductance term, should be avoided and replaced by concepts-based first on field observations and only then incorporated into numerical models.

6. Conclusions

Factors affecting river-aquifer interactions along a reach of the Namoi River in semiarid eastern Australia were investigated using a comparison between temperature-derived riverbed Darcy fluxes and reach losses from differential river gauging. The study includes highly transient conditions and longer time periods compared to previous studies. The results show slightly gaining to slightly losing conditions during low flows, to strongly losing conditions (i.e., increasing riverbed Darcy fluxes) driven primarily by increases in the river stage. The reach water balance, determined by differential river gauging, reveals that the increase in riverbed flux during high flows, which occur only 11% of the time, accounts for nearly 64% (or 43% when overbank events are excluded) of the reach losses.

A second factor that may influence variations in the riverbed fluxes examined here is hydraulic conductivity. Although variations in river stage can account for most of the flux variations, large differences in peak losses were observed during an event between the point measurements. It is suggested that this spatial variation in Darcy riverbed flux magnitude is driven by variations in hydraulic conductivity throughout the reach, and becomes increasingly significant during high flows.

Using the differential river gauging data, the relationships between the total flow volume, river stage, duration, and reach losses were examined. It was found that not only are the total flow volume, river stage and duration important in determining the volume of reach loss, but other factors play a significant role, several of which were hypothesized, but all of which require further investigation to resolve.

This study has implications for the conceptual understanding of river-aquifer interactions. Given the large spatial and temporal variations observed in riverbed fluxes for both low and high-flow conditions, it is reasonable to question any upscaling of point measurements to reach estimates, especially during high flows, which are not based upon a wider understanding of the catchment. The need to use field observations to drive conceptual generalizations made in numerical models (such as a spatially and temporally invariant conductance term) is also highlighted. Such simplifications, which lack "grounding" in field-based observations such as those made in this study, may well lead to inappropriately constrained models being used for water management decisions.

Acknowledgments
Funding for the research was provided by the Cotton Catchment Communities CRC (Projects 2.02.03 and 2.02.21). In-kind funding was provided by the National Centre for Groundwater Research and Training, an Australian Government initiative, supported by the Australian Research Council and the National Water Commission. Ian Cartwright, Peter Engesgaard, and three reviewers provided thoughtful comments on drafts of the paper. Rosemary Colacino reviewed a draft of the paper for readability.

References

ABS (2012), *Completing the Picture—Environmental Accounting in Practice*, Aust. Bur. of Stat., Canberra, ACT, Australia.
Andersen, M. S., and I. R. Acworth (2009), Stream aquifer interactions in the Maules Creek Catchment, Namoi Valley, NSW, Australia, *Hydrogeol. J.*, *17*, 2005–2021, doi:10.1007/s10040-009-0500-9.
Anderson, M. P. (2005), Heat as a ground water tracer, *Ground Water*, *43*(6), 951–968, doi:10.1111/j.1745-6584.2005.00052.x.
Angermann, L., J. Lewandowski, J. H. Fleckenstein, and G. Nützmann (2012), A 3D analysis algorithm to improve interpretation of heat pulse sensor results for the determination of small-scale flow directions and velocities in the hyporheic zone, *J. Hydrol.*, *475*, 1–11, doi:10.1016/j.jhydrol.2012.06.050.
Barlow, P. M., L. A. DeSimone, and A. F. Moench (2000), Aquifer response to stream-stage and recharge variations. II. Convolution method and applications, *J. Hydrol.*, *230*(3–4), 211–229, doi:10.1016/S0022-1694(00)00176-1.
Becker, M. W., T. Georgian, H. Ambrose, J. Siniscalchi, and K. Fredrick (2004), Estimating flow and flux of ground water discharge using water temperature and velocity, *J. Hydrol.*, *296*(1-4), 221–233, doi:10.1016/j.jhyrol.2004.03.025.
Bhaskar, A. S., J. W. Harvey, and E. J. Henry (2012), Resolving hyporheic and groundwater components of streambed water flux using heat as a tracer, *Water Resour. Res.*, *48*, W08524, doi:10.1029/2011WR011784.
Brunner, P., P. G. Cook, and C. T. Simmons (2009), Hydrogeologic controls on disconnection between surface water and groundwater, *Water Resour. Res.*, *45*, W01422, doi:10.1029/2008WR006953.
Buffington, J. M., and D. Tonina (2009), Hyporheic exchange in mountain rivers II: Effects of channel morphology on mechanics, scales, and rates of exchange, *Geogr. Compass*, *3*(3), 1038–1062, doi:10.1111/j.1749-8198.2009.00225.x.
Burrell, M., P. Moss, D. Green, A. Ali, and J. Petrovic (2011), *General Purpose Water Accounting Report 2009–2010: Namoi Catchment*, N. S. W. Off. of Water, Sydney.
Cardenas, M. B. (2009), Stream-aquifer interactions and hyporheic exchange in gaining and losing sinuous streams, *Water Resour. Res.*, *45*, W06429, doi:10.1029/2008WR007651.
Cardenas, M. B., and J. L. Wilson (2007), Effects of current-bed form induced fluid flow on the thermal regime of sediments, *Water Resour. Res.*, *43*, W08431, doi:10.1029/2006WR005343.
Cardenas, M. B., J. Wilson, and V. A. Zlotnik (2004), Impact of heterogeneity, bed forms, and stream curvature on subchannel hyporheic exchange, *Water Resour. Res.*, *40*, W08307, doi:10.1029/2004WR003008.
Constantz, J. (2008), Heat as a tracer to determine streambed water exchanges, *Water Resour. Res.*, *44*, W00D10, doi:10.1029/2008WR006996.
Constantz, J., M. H. Cox, and G. W. Su (2003), Comparison of heat and bromide as ground water tracers near streams, *Ground Water*, *41*(5), 647–656.
Cook, P. G. (2012), Estimating groundwater discharge to rivers from river chemistry surveys, *Hydrol. Processes*, *27*, 3694–3707, doi:10.1002/hyp.9493.
Cuthbert, M. O., and R. Mackay (2013), Impacts of nonuniform flow on estimates of vertical streambed flux, *Water Resour. Res.*, *49*, 19–28, doi:10.1029/2011wr011587.
Dahan, O., Y. Shani, Y. Enzel, Y. Yechieli, and A. Yakirevich (2007), Direct measurements of floodwater infiltration into shallow alluvial aquifers, *J. Hydrol.*, *344*(3-4), 157–170, doi:10.1016/j.jhydrol.2007.06.033.
de Vries, J. J., and I. Simmers (2002), Groundwater recharge: an overview of processes and challenges, *Hydrogeol. J.*, *10*(1), 5–17.
Desilets, S. L., T. Ferré, and P. A. Troch (2008), Effects of stream-aquifer disconnection on local flow patterns, *Water Resour. Res.*, *44*, W09501, doi:10.1029/2007WR006782.
DNR (2011), Surface Water Hydrograph Database, Dep. of Nat. Resour., NSW, Australia.
Doble, R. C., R. S. Crosbie, B. D. Smerdon, L. Peeters, and F. J. Cook (2012), Groundwater recharge from overbank floods, *Water Resour. Res.*, *48*, W09522, doi:10.1029/2011WR011441.
Ferguson, G., and V. Bense (2011), Uncertainty in 1D heat-flow analysis to estimate groundwater discharge to a stream, *Ground Water*, *49*, 336–347, doi:10.1111/j.1745-6584.2010.00735.x.
Fleckenstein, J. H., R. G. Niswonger, and G. E. Fogg (2006), River-aquifer interactions, geologic heterogeneity, and low-flow management, *Ground Water*, *44*, 837–852.
Genereux, D. P., S. Leahy, H. Mitasova, C. D. Kennedy, and D. R. Corbett (2008), Spatial and temporal variability of streambed hydraulic conductivity in West Bear Creek, North Carolina, USA, *J. Hydrol.*, *358*(3-4), 332–353.
Giambastiani, B., A. McCallum, M. Andersen, B. Kelly, and R. Acworth (2012), Understanding groundwater processes by representing aquifer heterogeneity in the Maules Creek Catchment, Namoi Valley (New South Wales, Australia), *Hydrogeol. J.*, *20*(6), 1027–1044.

Harvey, J. W., and B. J. Wagner (2000), Quantifying hydrologic interactions between streams and their subsurface hyporheic zones, in *Streams and Groundwaters*, edited by J. B. Jones and P. J. Mulholland, pp. 9–10, Academic, San Diego, Calif.
Hatch, C. E., A. T. Fisher, J. S. Revenaugh, J. Constantz, and C. Ruehl (2006), Quantifying surface water-groundwater interactions using time series analysis of streambed thermal records: Method development, *Water Resour. Res.*, *42*, W10410, doi:10.1029/2005WR004787.
Hatch, C. E., A. T. Fisher, C. R. Ruehl, and G. Stemler (2010), Spatial and temporal variations in streambed hydraulic conductivity quantified with time-series thermal methods, *J. Hydrol.*, *389*(3-4), 276–288, doi:10.1016/j.jhydrol.2010.05.046.
Hyun, Y., H. Kim, S.-S. Lee, and K.-K. Lee (2011), Characterizing streambed water fluxes using temperature and head data on multiple spatial scales in Munsan stream, South Korea, *J. Hydrol.*, *402*(3–4), 377–387.
Jolly, I. D., G. R. Walker, and K. A. Narayan (1994), Floodwater recharge processes in the Chowilla anabranch system, South Australia, *Soil Res.*, *32*(3), 417–435.
Jones, J. B., and P. J. Mulholland (2000), Streams and ground waters, *Ecology*, *88*, 727–731.
Kalbus, E., F. Reinstorf, and M. Schirmer (2006), Measuring methods for groundwater—Surface water interactions: A review, *Hydrol. Earth Syst. Sci.*, *10*(6), 873–887.
Kennedy, C. D., D. P. Genereux, H. Mitasova, D. R. Corbett, and S. Leahy (2008), Effect of sampling density and design on estimation of streambed attributes, *J. Hydrol.*, *355*(1), 164–180.
Lautz, L. K. (2010), Impacts of nonideal field conditions on vertical water velocity estimates from streambed temperature time series, *Water Resour. Res.*, *46*, W01509, doi:10.1029/2009WR007917.
Lautz, L. K. (2012), Observing temporal patterns of vertical flux through streambed sediments using time-series analysis of temperature records, *J. Hydrol.*, *464–465*, 199–215, doi:10.1016/j.jhydrol.2012.07.006.
Lautz, L. K., and R. E. Ribaudo (2012), Scaling up point-in-space heat tracing of seepage flux using bed temperatures as a quantitative proxy, *Hydrogeol. J.*, *20*(7), 1223–1238, doi:10.1007/s10040-012-0870-2.
Lerner, D. N., A. S. Issar, and I. Simmers (1990), Groundwater Recharge—A Guide to Understanding and Estimating Natural Recharge, Int. Assoc. of Hydrogeol., Kenilworth, U. K.
McCallum, A. M., M. S. Andersen, G. C. Rau, and R. I. Acworth (2012a), A 1-D analytical method for estimating surface water–groundwater interactions and effective thermal diffusivity using temperature time series, *Water Resour. Res.*, *48*, W11532, doi:10.1029/2012WR012007.
McCallum, A. M., M. S. Andersen, B. M. S. Giambastiani, B. F. J. Kelly, and R. I Acworth (2013), River–aquifer interactions in a semi-arid environment stressed by groundwater abstraction, *Hydrol. Processes*, *27*(7), 1072–1085, doi:10.1002/hyp.9229.
McCallum, A. M., M. S. Andersen, and R. I. Acworth (2014), A new method for estimating recharge to unconfined aquifers using differential river gauging, *Ground Water*, doi:10.1111/gwat.12046.
McCallum, J. L., P. G. Cook, D. Berhane, C. Rumpf, and G. A. McMahon (2012b), Quantifying groundwater flows to streams using differential flow gaugings and water chemistry, *J. Hydrol.*, *416*, 118–132.
MDBA (2010), *Guide to the Proposed Basin Plan: Technical Background*, Murray–Darling Basin Auth., Canberra.
Mutiti, S., and J. Levy (2010), Using temperature modeling to investigate the temporal variability of riverbed hydraulic conductivity during storm events, *J. Hydrol.*, *388*(3-4), 321–334, doi:10.1016/j.jhydrol.2010.05.011.
Rau, G. C., M. S. Andersen, A. M. McCallum, R. I. Acworth (2010), Analytical methods that use natural heat as a tracer to quantify surface water-groundwater exchange, evaluated using field temperature records, *Hydrogeol. J.*, *18*, 1093–1110, doi: 10.1007/s10040-010-0586-0.
Rau, G. C., M. S. Andersen, R. I. Acworth (2012a), Experimental investigation of the thermal dispersivity term and its significance in the heat transport equation for flow in sediments, *Water Resour. Res.*, *48*, W03511, doi: 10.1029/2011WR011038.
Rau, G. C., M. S. Andersen, R. I. Acworth (2012b), Experimental investigation of the thermal time-series method for surface water-groundwater interactions, *Water Resour. Res.*, *48*, W03530, doi: 10.1029/2011WR011560.
Rosenberry, D. O., and J. W. LaBaugh (2008), *Field Techniques for Estimating Water Fluxes Between Surface Water and Ground Water, Techniques and Methods 4–D2*, pp. 17, U.S. Geol. Surv., Denver, Colo.
Roshan, H., G. C. Rau, M. S. Andersen, and I. R. Acworth (2012), Use of heat as tracer to quantify vertical streambed flow in a 2-D flow field, *Water Resour. Res.*, *48*, W10508, doi:10.1029/2012WR011918.
Ruehl, C., A. T. Fisher, C. Hatch, M. Los Huertos, G. Stemler, and C. Shennan (2006), Differential gauging and tracer tests resolve seepage fluxes in a strongly-losing stream, *J. Hydrol.*, *330*(1-2), 235–248.
Scanlon, B. R., R. W. Healy, and P. G. Cook (2002), Choosing appropriate techniques for quantifying groundwater recharge, *Hydrogeol. J.*, *10*(1), 18–39.
Schornberg, C., C. Schmidt, E. Kalbus, and J. H. Fleckenstein (2010), Simulating the effects of geologic heterogeneity and transient boundary conditions on streambed temperatures—Implications for temperature-based water flux calculations, *Adv. Water Resour.*, *33*, 1309–1319, doi:10.1016/j.advwatres.2010.04.007.
Shanafield, M., C. Hatch, and G. Pohll (2011), Uncertainty in thermal time series analysis estimates of streambed water flux, *Water Resour. Res.*, *47*, W03504, doi:10.1029/2010WR009574.
Shentsis, I., and E. Rosenthal (2003), Recharge of aquifers by flood events in an arid region, *Hydrol. Processes*, *17*(4), 695–712, doi:10.1002/hyp.1160.
Shentsis, I., L. Meirovich, A. Ben-Zvi, and E. Rosenthal (1999), Assessment of transmission losses and groundwater recharge from runoff events in a wadi under shortage of data on lateral inflow, Negev, Israel, *Hydrol. Processes*, *13*(11), 1649–1663.
Soto-López, C. D., T. Meixner, and T. P. A. Ferré (2011), Effects of measurement resolution on the analysis of temperature time series for stream-aquifer flux estimation, *Water Resour. Res.*, *47*, W12602, doi:10.1029/2011WR010834.
Springer, A. E., W. D. Petroutson, and B. A. Semmens (1999), Spatial and temporal variability of hydraulic conductivity in active reattachment bars of the Colorado River, Grand Canyon, *Ground Water*, *37*(3), 338–344.
Storey, R. G., K. W. F. Howard, and D. D. Williams (2003), Factors controlling riffle- scale hyporheic exchange flows and their seasonal changes in a gaining stream: A three-dimensional groundwater flow model, *Water Resour. Res.*, *39*(2), 1034, doi:10.1029/2002WR001367.
Su, G. W., J. Jasperse, D. Seymour, and J. Constantz (2004), Estimation of hydraulic conductivity in an alluvial system using temperatures, *Ground Water*, *42*(6–7), 890–901.
Suzuki, S. (1960), Percolation measurements based on heat flow through soil with special reference to paddy fields, *J. Geophys. Res.*, *65*(9), 2883–2885.
Ward, A. S., M. Fitzgerald, M. N. Gooseff, T. J. Voltz, A. M. Binley, and K. Singha (2012), Hydrologic and geomorphic controls on hyporheic exchange during base flow recession in a headwater mountain stream, *Water Resour. Res.*, *48*, W04513, doi:10.1029/2011WR011461.
Winter, T. C., J. W. Harvey, O. L. Franke, and W. M. Alley (1998), Groundwater and surface water: A single resource, *USGS Circ. 1139*, U.S. Geol. Surv., Denver, Colo.